EXTENDED DISPLACEMENT DISCONTINUITY METHOD FOR CRACK ANALYSIS IN THREE-DIMENSIONAL TWO-PHASE TRANSVERSELY ISOTROPIC MAGNETOELECTROELASTIC MEDIA

Minghao Zhao, Na Li, Cuiying Fan and Tong Liu

EXTENDED DISPLACEMENT DISCONTINUITY METHOD FOR CRACK ANALYSIS IN THREE-DIMENSIONAL TWO-PHASE TRANSVERSELY ISOTROPIC MAGNETOELECTROELASTIC MEDIA

MINGHAO ZHAO, NA LI, CUIYING FAN AND TONG LIU

Green's functions for extended displacement discontinuity in a three-dimensional two-phase transversely isotropic magnetoelectroelastic medium are obtained by using the integral equation method. Based on the obtained Green's functions, an extended displacement discontinuity method is developed for analysis of planar cracks of arbitrary shape in three-dimensional two-phase magnetoelectroelastic media. A rectangular interior crack parallel to the interface under the electrically and magnetically impermeable boundary condition is analyzed, and the extended intensity factors are calculated by the proposed method. The magnetoelectroelastic medium is made with $BaTiO_3$ as the inclusion and $CoFe_2O_4$ as the matrix. The influences of the interface and the material properties on the extended intensity factors are studied. Numerical results show that the three normalized extended intensity factors, that is, the stress intensity factor, the electric displacement intensity factor, and the magnetic induction intensity factor, are different both from each other and from the case of a crack in a homogeneous medium.

1. Introduction

Because of the coupling effect among the mechanical, electrical and magnetic properties, magnetoelectroelastic materials are finding more and more applications in many areas such as electronics, lasers, supersonics, infrared, and microwave sources. Laminated composite structures of these materials are often used to enhance the coupling effects. The integrity and reliability of the structures depend greatly on the defects, such as inclusion, void, crack, etc., in the materials and structures. So the study of cracks in magnetoelectroelastic materials and structures has been attracting more and more efforts [Huang and Kuo 1997; Wang and Shen 2003; Wang and Mai 2003; Gao and Noda 2004; Zhou et al. 2004; Tian and Rajapakse 2005; Zhao et al. 2006a; Zhao et al. 2006b].

It is difficult to find the analytical solution of a problem in a general case. Numerical approaches have to be used such as the finite element method (FEM) and the boundary element method (BEM). BEM is one of the preferred techniques for dealing with field concentration and singularity problems in fracture mechanics. In this method, the Green's function or a fundamental solution plays an important role. A lot of work has been done in this field. In two-dimensional problems, for example, Chung and Ting [1995] gave the two-dimensional Green's functions for anisotropic magnetoelectroelastic media with an

elliptic hole or rigid inclusion. Based on the Stroh formalism, Jiang and Pan [2004] obtained the two-dimensional Green's functions in an exact closed form for general inclusion problems of anisotropic and fully coupled magnetoelectroelastic full, half, and bimaterial planes. Liu and Liu [2001] derived the Green's functions for an infinite two-dimensional anisotropic magnetoelectroelastic medium including an elliptical cavity by use of the technique of conformal mapping and the Laurent series expansions. Qin [2004] derived the Green's function for magnetoelectroelastic solids with an arbitrarily oriented half-plane or bimaterial interface. Ding et al. [2005] obtained the Green's functions for two-phase transversely isotropic magnetoelectroelastic media, including the two-dimensional Green's functions of an infinite plane and an infinite half-plane as well as the three-dimensional counterparts.

In three-dimensional problems, Pan [2002] obtained the three-dimensional Green's functions in anisotropic infinite, semiinfinite, and two-phase magnetoelectroelastic media based on extended Stroh formalism. Hou et al. [2005] presented the three-dimensional Green's functions of infinite, two-phase, and semiinfinite transversely isotropic magnetoelectroelastic media under point forces, point charge, and magnetic monopole in terms of elementary functions for all cases of distinct eigenvalues and multiple eigenvalues. Wang and Shen [2002] gave the general solutions and the fundamental solutions or Green's functions for magnetoelectroelastic media through five potential functions.

Parallel to the Green's functions for point force, the displacement discontinuity fundamental solutions [Crouch 1976] are other important kinds of Green's functions, which are of special use in displacement discontinuity boundary integral equation methods in fracture mechanics. This method is commonly called displacement discontinuity method (DDM). It has been proved to be one of the most powerful methods in fracture mechanics of purely elastic media [Wen 1996; Pan and Amadei 1996; Zhao et al. 1998], poroelastic media [Pan 1991], as well as for piezoelectric media [Zhao et al. 1997a; Zhao et al. 1997b; Zhao et al. 2004]. In the present paper, the Green's functions for the extended displacement discontinuity in three-dimensional two-phase transversely isotropic magnetoelectroelastic media will be derived. Based on the obtained Green's function, the extended Crouch fundamental solutions for uniformly distributed extended displacement discontinuity on a rectangular segment are obtained and the extended displacement discontinuity method is proposed. A rectangular crack is analyzed by the proposed method as an application.

2. Basic equation

In the absence of body force, electric charge, and electric current, the basic equations for a three-dimensional two-phase transversely isotropic magnetoelectroelastic medium with the poling direction being along the z-direction in the $oxyz$ Cartesian coordinate system are given by

$$\sigma_{ij,j} = 0, \qquad D_{i,i} = 0, \qquad B_{i,i} = 0, \tag{1a}$$

$$\begin{aligned}
\sigma_{ij} &= c_{ijkl}(u_{k,l} + u_{l,k})/2 + e_{kij}\varphi_{,k} + f_{kij}\psi_{,k}, \\
D_i &= e_{ikl}(u_{k,l} + u_{l,k})/2 - \varepsilon_{ik}\varphi_{,k} - g_{ik}\psi_{,k}, \\
B_i &= f_{ikl}(u_{k,l} + u_{l,k})/2 - g_{ik}\varphi_{,k} - \mu_{ik}\psi_{,k},
\end{aligned} \tag{1b}$$

where $i, j = 1, 2, 3(x, y, z)$, and σ_{ij}, D_i, and B_i are the stress, electric displacement, and magnetic induction components, respectively. u_i is the displacement component, and φ and ψ are respectively
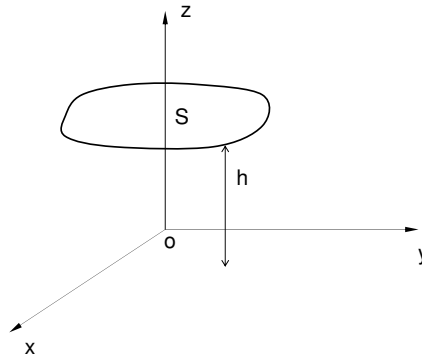
Figure 1. An arbitrarily shaped planar crack S in the $z = h(h > 0)$ plane in a magneto-electroelastic bimaterial.

the electric potential and magnetic potential. c_{ij}, e_{kij}, f_{kij}, ε_{ij}, g_{ij} and μ_{ij} are the elastic constant, piezo-electric constant, piezomagnetic constant, dielectric permittivity, electromagnetic constant, and magnetic permeability, respectively. A subscript comma denotes the partial differentiation with respect to the coordinate.

3. Boundary integral expressions of extended displacement discontinuity

Consider a three-dimensional two-phase transversely isotropic magnetoelectroelastic medium with the interface being parallel to the plane of isotropy. A Cartesian coordinate system is set up such that the xoy-plane lies in the interface. A planar crack S of arbitrary shape lies in the plane $z = h(h > 0)$ as shown in Figure 1. The upper and lower surfaces of S are denoted by S^+ and S^-, respectively. The outer normal vectors of S^+ and S^- are respectively given by

$$\{n_i\}^+ = \{0, 0, -1\}, \qquad \{n_i\}^- = \{0, 0, 1\}. \tag{2}$$

The prescribed tractions, the electric displacement boundary value, and the magnetic induction boundary value on the crack faces are denoted respectively by p_i ($i = 1, 2, 3$, or x, y, z), ω, and γ, which hereafter are called extended tractions. By using the extended point force fundamental solutions given in Appendix A and the Somigliana identity for magnetoelectroelastic media, the displacements u_i, the electric potential φ, and the magnetic potential ψ at any internal point (x, y, z) can be expressed in the following forms

$$u_i(x, y, z) = -\int_{S^+} [P_{ij}^F u_j + \Omega_i^F \varphi + \Gamma_i^F \psi] dS - \int_{S^-} [P_{ij}^F u_j + \Omega_i^F \varphi + \Gamma_i^F \psi] dS$$
$$+ \int_{S^+} [p_j U_{ij}^F + \omega \Phi_i^F + \gamma \Psi_i^F] dS + \int_{S^-} [p_j U_{ij}^F + \omega \Phi_i^F + \gamma \Psi_i^F] dS, \tag{3}$$

$$-\varphi(x, y, z) = -\int_{S^+} [P_j^D u_j + \Omega^D \varphi + \Gamma^D \psi] dS - \int_{S^-} [P_j^D u_j + \Omega^D \varphi + \Gamma^D \psi] dS$$

$$+ \int_{S^+} [p_j U_j^D + \omega \Phi^D + \gamma \Psi^D] dS + \int_{S^-} [p_j U_j^D + \omega \Phi^D + \gamma \Psi^D] dS, \quad (4)$$

$$-\psi(x, y, z) = -\int_{S^+} [P_j^B u_j + \Omega^B \varphi + \Gamma^B \psi] dS - \int_{S^-} [P_j^B u_j + \Omega^B \varphi + \Gamma^B \psi] dS$$

$$+ \int_{S^+} [p_j U_j^B + \omega \Phi^B + \gamma \Psi^B] dS + \int_{S^-} [p_j U_j^B + \omega \Phi^B + \gamma \Psi^B] dS, \quad (5)$$

where P_{ij}^F, Ω_i^F, Γ_i^F, U_{ij}^F, Φ_i^F, and Ψ_i^F are the tractions, the electric displacement boundary value, the magnetic induction boundary value, the displacements, the electric potential, and the magnetic potential of the fundamental solutions corresponding to the unit point force in the ith direction, respectively, P_j^D, Ω^D, Γ^D, U_j^D, Φ^D, and Ψ^D corresponding to the unit point electric charge and P_j^B, Ω^B, Γ^B, U_j^B, Φ^B, and Ψ^B corresponding to the unit point electric current

$$\begin{aligned}
P_{ij}^F &= \sigma_{ijk}^F n_k, & \Omega_i^F &= D_{ik}^F n_k, & \Gamma_i^F &= B_{ik}^F n_k, \\
P_j^D &= \sigma_{jk}^D n_k, & \Omega^D &= D_k^D n_k, & \Gamma^D &= B_k^D n_k, \\
P_j^B &= \sigma_{jk}^B n_k, & \Omega^B &= D_k^B n_k, & \Gamma^B &= B_k^B n_k,
\end{aligned} \quad (6)$$

where the upper index F, D, and B refer to the variables corresponding to point forces, point electric charge, and point electric current, respectively. Based on the fundamental solutions, we easily obtain the following relationship on the crack faces

$$\begin{aligned}
P_{ij}^F|_{S^+} &= -P_{ij}^F|_{S^-}, & U_{ij}^F|_{S^+} &= U_{ij}^F|_{S^-}, & \Omega_i^F|_{S^+} &= -\Omega_i^F|_{S^-}, \\
\Phi_i^F|_{S^+} &= \Phi_i^F|_{S^-}, & \Gamma_i^F|_{S^+} &= -\Gamma_i^F|_{S^-}, & \Psi_i^F|_{S^+} &= \Psi_i^F|_{S^-} \\
P_j^D|_{S^+} &= -P_j^D|_{S^-}, & U_j^D|_{S^+} &= U_j^D|_{S^-}, & \Omega^D|_{S^+} &= -\Omega^D|_{S^-}, \\
\Phi^D|_{S^+} &= \Phi^D|_{S^-}, & \Gamma^D|_{S^+} &= -\Gamma^D|_{S^-}, & \Psi^D|_{S^+} &= \Psi^D|_{S^-}, \\
P_j^B|_{S^+} &= -P_j^B|_{S^-}, & U_j^B|_{S^+} &= U_j^B|_{S^-}, & \Omega^B|_{S^+} &= -\Omega^B|_{S^-}, \\
\Phi^B|_{S^+} &= \Phi^B|_{S^-}, & \Gamma^B|_{S^+} &= -\Gamma^B|_{S^-}, & \Psi^B|_{S^+} &= \Psi^B|_{S^-}.
\end{aligned}$$

On assuming that the extended tractions on the upper and lower crack faces satisfy the conditions

$$p_i|_{S^+} = -p_i|_{S^-}, \qquad \omega|_{S^+} = -\omega|_{S^-}, \qquad \gamma|_{S^+} = -\gamma|_{S^-}, \quad (7)$$

and considering Equations (2) and (6)–(7), Equations (3)–(5) are reduced to

$$u_i(x, y, z) = -\int_{S^+} [P_{ij}^F \|u_j\| + \Omega_i^F \|\varphi\| + \Gamma_i^F \|\psi\|] dS(\xi, \eta),$$

$$-\varphi(x, y, z) = -\int_{S^+} [P_j^D \|u_j\| + \Omega^D \|\varphi\| + \Gamma^D \|\psi\|] dS(\xi, \eta), \quad (8)$$

$$-\psi(x, y, z) = -\int_{S^+} [P_j^B \|u_j\| + \Omega^B \|\varphi\| + \Gamma^B \|\psi\|] dS(\xi, \eta).$$
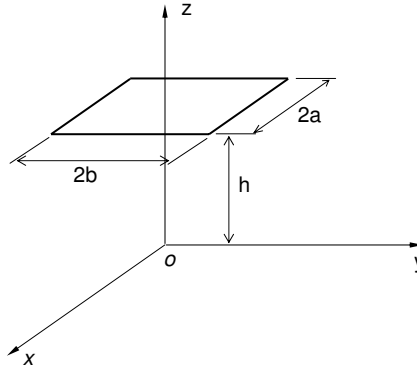
Figure 2. A rectangular crack in the plane $z = h(h > 0)$ in a magnetoelectroelastic bimaterial.

In Equation (8), $\|u_i\|$, $\|\varphi\|$, and $\|\psi\|$ are respectively the displacement discontinuities, the electric potential discontinuity, and the magnetic potential discontinuity across the crack faces, which are called the extended displacement discontinuities and given by:

$$\|u_i(\xi, \eta)\| = u_i(\xi, \eta, h^+) - u_i(\xi, \eta, h^-), \quad \|\varphi(\xi, \eta)\| = \varphi(\xi, \eta, h^+) - \varphi(\xi, \eta, h^-),$$
$$\|\psi(\xi, \eta)\| = \psi(\xi, \eta, h^+) - \psi(\xi, \eta, h^-).$$

In the following derivations, the displacement components are also denoted by $u = u_x$, $v = u_y$, $w = u_z$, and the following symbols will be used

$$z_i = s_i z, \quad \zeta_i = s_i h, \quad z_{ij} = h_i + z_j,$$
$$R_{ij} = \sqrt{(\xi - x)^2 + (\eta - y)^2 + z_{ij}^2}, \quad \bar{z}_{ij} = h_i - z_j,$$
$$\bar{R}_{ij} = \sqrt{(\xi - x)^2 + (\eta - y)^2 + \bar{z}_{ij}^2}, \quad \tilde{R}_{ij} = R_{ij} + z_{ij},$$
$$\hat{R}_{ij} = \bar{R}_{ij} - \bar{z}_{ij}, \quad (i, j = 1, 2, 3, 4, \text{ and } i = j = 5),$$

where s_i are material constants, which are given in Appendix A.

4. Green's functions for unit extended point displacement discontinuities

Assume that the planar crack S is a rectangle of length $2a = 2b$ with the center being at point $(0, 0, h)$, as shown in Figure 2.

The fundamental solutions corresponding to extended displacement discontinuities should satisfy the governing equations of magnetoelectroelastic media subject, respectively, to the following conditions:

$$\lim_{a \to 0} \int_S \{\|u\|, \|v\|, \|w\|, \|\varphi\|, \|\psi\|\} dS = \{1, 0, 0, 0, 0\}, \tag{9a}$$

$$\lim_{a \to 0} \int_S \{\|u\|, \|v\|, \|w\|, \|\varphi\|, \|\psi\|\} dS = \{0, 1, 0, 0, 0\}, \tag{9b}$$

$$\lim_{a \to 0} \int_S \{\|u\|, \|v\|, \|w\|, \|\varphi\|, \|\psi\|\} dS = \{0, 0, 1, 0, 0\}, \tag{9c}$$

$$\lim_{a \to 0} \int_S \{\|u\|, \|v\|, \|w\|, \|\varphi\|, \|\psi\|\} dS = \{0, 0, 0, 1, 0\}, \tag{9d}$$

$$\lim_{a \to 0} \int_S \{\|u\|, \|v\|, \|w\|, \|\varphi\|, \|\psi\|\} dS = \{0, 0, 0, 0, 1\}. \tag{9e}$$

4.1. *Green's function satisfying Equation* (9a)*.* On the plane $z = h(h > 0)$, the discontinuity boundary condition in the x-axis direction is indeed the Dirac δ-function

$$\|u(\xi, \eta)\| = \delta(\xi, \eta). \tag{10}$$

Inserting Equations (9a) and (10) and the fundamental solutions for extended point force in Appendix A into Equation (8) yields

$$u = -\omega_{51} \left[D_5 \left(\frac{1}{\bar{R}_{55}\hat{R}_{55}} - \frac{y^2}{\bar{R}_{55}^3\hat{R}_{55}} - \frac{y^2}{\bar{R}_{55}^2\hat{R}_{55}^2} \right) - D_{55} \left(\frac{1}{R_{55}\tilde{R}_{55}} - \frac{y^2}{R_{55}^3\tilde{R}_{55}} - \frac{y^2}{R_{55}^2\tilde{R}_{55}^2} \right) \right]$$
$$+ \sum_{i=1}^{4} \omega_{i1} \left[D_i \left(\frac{1}{\bar{R}_{ii}\hat{R}_{ii}} - \frac{x^2}{\bar{R}_{ii}^3\hat{R}_{ii}} - \frac{x^2}{\bar{R}_{ii}^2\hat{R}_{ii}^2} \right) - \sum_{j=1}^{4} D_{ij} \left(\frac{1}{R_{ij}\tilde{R}_{ij}} - \frac{x^2}{R_{ij}^3\tilde{R}_{ij}} - \frac{x^2}{R_{ij}^2\tilde{R}_{ij}^2} \right) \right], \tag{11}$$

$$v = -xy\omega_{51} \left[D_5 \left(\frac{1}{\bar{R}_{55}^3\hat{R}_{55}} + \frac{1}{\bar{R}_{55}^2\hat{R}_{55}^2} \right) - D_{55} \left(\frac{1}{R_{55}^3\tilde{R}_{55}} + \frac{1}{R_{55}^2\tilde{R}_{55}^2} \right) \right]$$
$$- xy \sum_{i=1}^{4} \omega_{i1} \left[D_i \left(\frac{1}{\bar{R}_{ii}^3\hat{R}_{ii}} + \frac{1}{\bar{R}_{ii}^2\hat{R}_{ii}^2} \right) - \sum_{j=1}^{4} D_{ij} \left(\frac{1}{R_{ij}^3\tilde{R}_{ij}} + \frac{1}{R_{ij}^2\tilde{R}_{ij}^2} \right) \right], \tag{12}$$

$$w = -x \sum_{i=1}^{4} \omega_{i1} \left(\frac{A_i}{\bar{R}_{ii}^3} - \sum_{j=1}^{4} \frac{A_{ij}}{R_{ij}^3} \right), \qquad \varphi = x \sum_{i=1}^{4} \omega_{i1} \left(\frac{B_i}{\bar{R}_{ii}^3} - \sum_{j=1}^{4} \frac{B_{ij}}{R_{ij}^3} \right), \tag{13}$$

$$\psi = x \sum_{i=1}^{4} \omega_{i1} \left(\frac{C_i}{\bar{R}_{ii}^3} - \sum_{j=1}^{4} \frac{C_{ij}}{R_{ij}^3} \right). \tag{14}$$

Substituting Equations (11)–(14) into the constitutive Equation (1b) yields the stress, electric displacement, and magnetic induction

$$
\sigma_{yz} = 3xy \left\{ c_{44}\omega_{51}\left(D_5 \frac{s_5}{\bar{R}_{55}^5} - D_{55}\frac{s_5}{R_{55}^5} \right) + c_{44}\sum_{i=1}^{4}\omega_{i1}\left(D_i \frac{s_i}{\bar{R}_{ii}^5} - \sum_{j=1}^{4} D_{ij}\frac{s_j}{R_{ij}^5} \right) \right.
$$
$$
\left. + \sum_{i=1}^{4}\omega_{i1}\left[(c_{44}A_i - e_{15}B_i - f_{15}C_i)\frac{1}{\bar{R}_{ii}^5} - \sum_{j=1}^{4}(c_{44}A_{ij} - e_{15}B_{ij} - f_{15}C_{ij})\frac{1}{R_{ij}^5} \right] \right\}, \quad (15)
$$

$$
\sigma_{xz} = c_{44}\left\{ \omega_{51}s_5\left[D_5\left(\frac{1}{\bar{R}_{55}^3} - y^2\frac{3}{\bar{R}_{55}^5}\right) - D_{55}\left(\frac{1}{R_{55}^3} - y^2\frac{3}{R_{55}^5}\right) \right] \right.
$$
$$
\left. + \sum_{i=1}^{4}\omega_{i1}\left[-D_i s_i\left(\frac{1}{\bar{R}_{ii}^3} - x^2\frac{3}{\bar{R}_{ii}^5}\right) + \sum_{j=1}^{4} D_{ij}s_j\left(\frac{1}{R_{ij}^3} - x^2\frac{3}{R_{ij}^5}\right) \right] \right\}
$$
$$
- \sum_{i=1}^{4}\omega_{i1}\left[(c_{44}A_i - e_{15}B_i - f_{15}C_i)\left(\frac{1}{\bar{R}_{ii}^3} - \frac{3x^2}{\bar{R}_{ii}^5}\right) \right.
$$
$$
\left. - \sum_{j=1}^{4}(c_{44}A_{ij} - e_{15}B_{ij} - f_{15}C_{ij})\left(\frac{1}{R_{ij}^3} - \frac{3x^2}{R_{ij}^5}\right) \right], \quad (16)
$$

$$
\sigma_{zz} = -4c_{13}x \sum_{i=1}^{4}\omega_{i1}\left[D_i\left(\frac{1}{\bar{R}_{ii}^3\hat{R}_{ii}} + \frac{1}{\bar{R}_{ii}^2\hat{R}_{ii}^2}\right) - \sum_{j=1}^{4} D_{ij}\left(\frac{1}{R_{ij}^3\tilde{R}_{ij}} + \frac{1}{R_{ij}^2\tilde{R}_{ij}^2}\right) \right]
$$
$$
+ (x^2 + y^2)xc_{13}\sum_{i=1}^{4}\omega_{i1}\left[D_i\left(\frac{3}{\bar{R}_{ii}^5\hat{R}_{ii}} + \frac{3}{\bar{R}_{ii}^4\hat{R}_{ii}^2} + \frac{2}{\bar{R}_{ii}^3\hat{R}_{ii}^3}\right) - \sum_{j=1}^{4} D_{ij}\left(\frac{3}{R_{ij}^5\tilde{R}_{ij}} + \frac{3}{R_{ij}^4\tilde{R}_{ij}^2} + \frac{2}{R_{ij}^3\tilde{R}_{ij}^3}\right) \right]
$$
$$
- x\sum_{i=1}^{4}3\omega_{i1}\left[\frac{s_iz_{ii}}{\bar{R}_{ii}^5}(c_{33}A_i - e_{33}B_i - f_{33}C_i) + \sum_{j=1}^{4} \frac{s_jz_{ij}}{R_{ij}^5}(c_{33}A_{ij} - e_{33}B_{ij} - f_{33}C_{ij}) \right], \quad (17)
$$

$$
D_z = -4e_{31}x \sum_{i=1}^{4}\omega_{i1}\left[D_i\left(\frac{1}{\bar{R}_{ii}^3\hat{R}_{ii}} + \frac{1}{\bar{R}_{ii}^2\hat{R}_{ii}^2}\right) - \sum_{j=1}^{4} D_{ij}\left(\frac{1}{R_{ij}^3\tilde{R}_{ij}} + \frac{1}{R_{ij}^2\tilde{R}_{ij}^2}\right) \right]
$$
$$
+ (x^2 + y^2)xe_{31}\sum_{i=1}^{4}\omega_{i1}\left[D_i\left(\frac{3}{\bar{R}_{ii}^5\hat{R}_{ii}} + \frac{3}{\bar{R}_{ii}^4\hat{R}_{ii}^2} + \frac{2}{\bar{R}_{ii}^3\hat{R}_{ii}^3}\right) - \sum_{j=1}^{4} D_{ij}\left(\frac{3}{R_{ij}^5\tilde{R}_{ij}} + \frac{3}{R_{ij}^4\tilde{R}_{ij}^2} + \frac{2}{R_{ij}^3\tilde{R}_{ij}^3}\right) \right]
$$
$$
- x\sum_{i=1}^{4}3\omega_{i1}\left[\frac{s_iz_{ii}}{\bar{R}_{ii}^5}(e_{33}A_i + \varepsilon_{33}B_i + g_{33}C_i) + \sum_{j=1}^{4} \frac{s_jz_{ij}}{R_{ij}^5}(e_{33}A_{ij} + \varepsilon_{33}B_{ij} + g_{33}C_{ij}) \right], \quad (18)
$$

$$
B_z = -4f_{31}x \sum_{i=1}^{4} \omega_{i1} \left[D_i \left(\frac{1}{\bar{R}_{ii}^3 \hat{R}_{ii}} + \frac{1}{\bar{R}_{ii}^2 \hat{R}_{ii}^2} \right) - \sum_{j=i}^{4} D_{ij} \left(\frac{1}{R_{ij}^3 \tilde{R}_{ij}} + \frac{1}{R_{ij}^2 \tilde{R}_{ij}^2} \right) \right]
$$

$$
+ (x^2 + y^2) x f_{31} \sum_{i=1}^{4} \omega_{i1} \left[D_i \left(\frac{3}{\bar{R}_{ii}^5 \hat{R}_{ii}} + \frac{3}{\bar{R}_{ii}^4 \hat{R}_{ii}^2} + \frac{2}{\bar{R}_{ii}^3 \hat{R}_{ii}^3} \right) - \sum_{j=1}^{4} D_{ij} \left(\frac{3}{R_{ij}^5 \tilde{R}_{ij}} + \frac{3}{R_{ij}^4 \tilde{R}_{ij}^2} + \frac{2}{R_{ij}^3 \tilde{R}_{ij}^3} \right) \right]
$$

$$
- x \sum_{i=1}^{4} 3\omega_{i1} \left[\frac{z_{ii} s_i}{\bar{R}_{ii}^5} (f_{33}A_i + g_{33}B_i + \mu_{33}C_i) + \sum_{j=1}^{4} \frac{z_{ij} s_j}{R_{ij}^5} (f_{33}A_{ij} + g_{33}B_{ij} + \mu_{33}C_{ij}) \right]. \quad (19)
$$

From above solutions, the Green's function corresponding to Equation (9b) can be easily obtained by coordinate transformation.

4.2. *Green's function satisfying Equation* (9c). On the crack face, the displacement discontinuity condition in the z-axis direction is

$$
\| w(\xi, \eta) \| = \delta(\xi, \eta). \quad (20)
$$

Inserting Equations (9c) and (20) and the fundamental solutions for extended point force in Appendix A into Equation (8) yields the extended displacements

$$
\begin{aligned}
u &= -x \sum_{i=1}^{4} \vartheta_{i1} \left[\frac{D_i}{\bar{R}_{ii}^3} + \sum_{j=1}^{4} \frac{D_{ij}}{R_{ij}^3} \right], \\
v &= -y \sum_{i=1}^{4} \vartheta_{i1} \left[\frac{D_i}{\bar{R}_{ii}^3} + \sum_{j=1}^{4} \frac{D_{ij}}{R_{ij}^3} \right], \\
w &= \sum_{i=1}^{4} \vartheta_{i1} \left[\frac{A_i (h_i - z_i)}{\bar{R}_{ii}^3} - \sum_{j=1}^{4} \frac{A_{ij} (h_i + z_j)}{R_{ij}^3} \right], \\
\varphi &= -\sum_{i=1}^{4} \vartheta_{i1} \left[\frac{B_i (h_i - z_i)}{\bar{R}_{ii}^3} - \sum_{j=1}^{4} \frac{B_{ij} (h_i + z_j)}{R_{ij}^3} \right], \\
\psi &= -\sum_{i=1}^{4} \vartheta_{i1} \left[\frac{C_i (h_i - z_i)}{\bar{R}_{ii}^3} - \sum_{j=1}^{4} \frac{C_{ij} (h_i + z_j)}{R_{ij}^3} \right].
\end{aligned} \quad (21)
$$

Similarly, the corresponding stress, electric displacement and magnetic induction are derived

$$
\sigma_{yz} = 3y \left\{ c_{44} \sum_{i=1}^{4} \vartheta_{i1} \left(-D_i \frac{s_i z_{ii}}{\bar{R}_{ii}^5} + \sum_{j=1}^{4} D_{ij} \frac{s_j z_{ij}}{R_{ij}^5} \right) - \sum_{i=1}^{4} \vartheta_{i1} \left[(c_{44}A_i - e_{15}B_i - f_{15}C_i) \frac{(h_i - z_i)}{\bar{R}_{ii}^5} \right. \right.
$$

$$
\left. \left. - \sum_{j=1}^{4} (c_{44}A_{ij} - e_{15}B_{ij} - f_{15}C_{ij}) \frac{(h_j + z_j)}{R_{ij}^5} \right] \right\}, \quad (22)
$$

$$\sigma_{xz} = 3x \left\{ c_{44} \sum_{i=1}^{4} \vartheta_{i1} \left(-D_i \frac{s_i z_{ii}}{\bar{R}_{ii}^5} + \sum_{j=1}^{4} D_{ij} \frac{s_j z_{ij}}{R_{ij}^5} \right) - \sum_{i=1}^{4} \vartheta_{i1} \left[\left(c_{44} A_i - e_{15} B_i - f_{15} C_i \right) \frac{(h_i - z_i)}{\bar{R}_{ii}^5} \right. \right.$$
$$\left. \left. - \sum_{j=1}^{4} \left(c_{44} A_{ij} - e_{15} B_{ij} - f_{15} C_{ij} \right) \frac{(h_j + z_j)}{R_{ij}^5} \right] \right\}, \quad (23)$$

$$\sigma_{zz} = \sum_{i=1}^{4} \vartheta_{i1} \left\{ c_{13} \left[D_i \left(-\frac{2}{\bar{R}_{ii}^3} + \frac{3(x^2 + y^2)}{\bar{R}_{ii}^5} \right) + \sum_{j=1}^{4} D_{ij} \left(-\frac{2}{R_{ij}^3} + \frac{3(x^2 + y^2)}{R_{ij}^5} \right) \right] \right.$$
$$- s_i \left(c_{33} A_i - e_{33} B_i - f_{33} C_i \right) \left(\frac{1}{\bar{R}_{ii}^3} - \frac{3z_i(h_i - z_i)}{\bar{R}_{ii}^5} \right)$$
$$\left. - \sum_{j=1}^{4} D_{ij} s_j \left(c_{33} A_{ij} - e_{33} B_{ij} - f_{33} C_{ij} \right) \left(\frac{1}{R_{ij}^3} - \frac{3z_j(h_i + z_j)}{R_{ij}^5} \right) \right\}, \quad (24)$$

$$D_z = \sum_{i=1}^{4} \vartheta_{i1} \left\{ e_{31} \left[D_i \left(-\frac{2}{\bar{R}_{ii}^3} + \frac{3(x^2 + y^2)}{\bar{R}_{ii}^5} \right) + \sum_{j=1}^{4} D_{ij} \left(-\frac{2}{R_{ij}^3} + \frac{3(x^2 + y^2)}{R_{ij}^5} \right) \right] \right.$$
$$- s_i \left(e_{33} A_i + \varepsilon_{33} B_i + g_{33} C_i \right) \left(\frac{1}{\bar{R}_{ii}^3} - \frac{3z_i(h_i - z_i)}{\bar{R}_{ii}^5} \right)$$
$$\left. - \sum_{j=1}^{4} D_{ij} s_j \left(e_{33} A_{ij} + \varepsilon_{33} B_{ij} + g_{33} C_{ij} \right) \left(\frac{1}{R_{ij}^3} - \frac{3z_j(h_i + z_j)}{R_{ij}^5} \right) \right\}, \quad (25)$$

$$B_z = \sum_{i=1}^{4} \vartheta_{i1} \left\{ f_{31} \left[D_i \left(-\frac{2}{\bar{R}_{ii}^3} + \frac{3(x^2 + y^2)}{\bar{R}_{ii}^5} \right) + \sum_{j=1}^{4} D_{ij} \left(-\frac{2}{R_{ij}^3} + \frac{3(x^2 + y^2)}{R_{ij}^5} \right) \right] \right.$$
$$- s_i \left(f_{33} A_i + g_{33} B_i + \mu_{33} C_i \right) \left(\frac{1}{\bar{R}_{ii}^3} - \frac{3z_i(h_i - z_i)}{\bar{R}_{ii}^5} \right)$$
$$\left. - \sum_{j=1}^{4} D_{ij} s_j \left(f_{33} A_{ij} + g_{33} B_{ij} + \mu_{33} C_{ij} \right) \left(\frac{1}{R_{ij}^3} - \frac{3z_j(h_i + z_j)}{R_{ij}^5} \right) \right\}. \quad (26)$$

The fundamental solutions corresponding to Equation (9d) and Equation (9e) can be obtained by taking ϑ_{i2} and ϑ_{i3} instead of ϑ_{i1}, respectively.

5. Extended crouch fundamental solution

In this section, the extended Crouch fundamental solutions are derived for a three-dimensional two-phase magnetoelectroelastic medium.

Consider a rectangular crack of length $2a$ and width $2b$ in the plane $z = h$. Uniformly distributed extended displacement discontinuities $\|u^e\|$, $\|v^e\|$, $\|w^e\|$, $\|\varphi^e\|$, and $\|\psi^e\|$ are applied on the crack faces. Integrating the extended displacement discontinuity Green's functions derived in last section on the rectangular crack with lengthy manipulations yields the extended stress fields

$$
\begin{aligned}
\sigma_{xz}^e = {}& \left(L_{X1}\bar{G}_{55}^{(1)} - L_{X2}G_{55}^{(1)}\right)\|u^e\| - \left(L_{X1}\bar{G}_{55}^{(3)} - L_{X2}G_{55}^{(3)}\right)\|v^e\| \\
& + \sum_{i=1}^{4}\left[\left(-L_{11}^i\bar{G}_{ii}^{(2)} + \sum_{j=1}^{4}L_{12}^{ij}G_{ij}^{(2)}\right)\|u^e\| - \left(L_{11}^i\bar{G}_{ii}^{(3)} - \sum_{j=1}^{4}L_{12}^{ij}G_{ij}^{(3)}\right)\|v^e\| \right. \\
& \qquad - \bar{G}_{ii}^{(4)}\left(L_{211}^i\|w^e\| + L_{212}^i\|\varphi^e\| + L_{213}^i\|\psi^e\|\right) \\
& \qquad \left. + \sum_{j=1}^{4}G_{ij}^{(4)}\left(L_{221}^{ij}\|w^e\| + L_{222}^{ij}\|\varphi^e\| + L_{223}^{ij}\|\psi^e\|\right)\right], \quad (27)
\end{aligned}
$$

$$
\begin{aligned}
\sigma_{yz}^e = {}& \left(L_{X1}\bar{G}_{55}^{(3)} - L_{X2}G_{55}^{(3)}\right)\|u^e\| - \left(L_{X1}\bar{G}_{55}^{(2)} - L_{X2}G_{55}^{(2)}\right)\|v^e\| \\
& + \sum_{i=1}^{4}\left[\left(L_{11}^i\bar{G}_{ii}^{(3)} - \sum_{j=1}^{4}L_{12}^{ij}G_{ij}^{(3)}\right)\|u^e\| + \left(L_{11}^i\bar{G}_{ii}^{(1)} - \sum_{j=1}^{4}L_{12}^{ij}G_{ij}^{(1)}\right)\|v^e\| \right. \\
& \qquad - \bar{G}_{ii}^{(5)}\left(L_{211}^i\|w^e\| + L_{212}^i\|\varphi^e\| + L_{213}^i\|\psi^e\|\right) \\
& \qquad \left. + \sum_{j=1}^{4}G_{ij}^{(5)}\left(L_{221}^{ij}\|w^e\| + L_{222}^{ij}\|\varphi^e\| + L_{223}^{ij}\|\psi^e\|\right)\right], \quad (28)
\end{aligned}
$$

$$
\begin{aligned}
\sigma_{zz}^e = {}& \sum_{i=1}^{4}\left[\left(-L_{Z1}^i\bar{G}_{ii}^{(4)} + \sum_{j=1}^{4}L_{Z2}^{ij}G_{ij}^{(4)}\right)\|u^e\| + \left(L_{Z1}^i\bar{G}_{ii}^{(5)} + \sum_{j=1}^{4}L_{Z2}^{ij}G_{ij}^{(5)}\right)\|v^e\| \right. \\
& \qquad + \bar{G}_{ii}^{(6)}\left(L_{Z11}^i\|w^e\| + L_{Z12}^i\|\varphi^e\| + L_{Z13}^i\|\psi^e\|\right) \\
& \qquad \left. + \sum_{j=1}^{4}G_{ij}^{(6)}\left(L_{Z21}^{ij}\|w^e\| + L_{Z22}^{ij}\|\varphi^e\| + L_{Z23}^{ij}\|\psi^e\|\right)\right], \quad (29)
\end{aligned}
$$

$$
\begin{aligned}
D_{z}^e = {}& \sum_{i=1}^{4}\left[\left(-L_{D1}^i\bar{G}_{ii}^{(4)} + \sum_{j=1}^{4}L_{D2}^{ij}G_{ij}^{(4)}\right)\|u^e\| + \left(L_{D1}^i\bar{G}_{ii}^{(5)} + \sum_{j=1}^{4}L_{D2}^{ij}G_{ij}^{(5)}\right)\|v^e\| \right. \\
& \qquad + \bar{G}_{ii}^{(6)}\left(L_{D11}^i\|w^e\| + L_{D12}^i\|\varphi^e\| + L_{D13}^i\|\psi^e\|\right) \\
& \qquad \left. + \sum_{j=1}^{4}G_{ij}^{(6)}\left(L_{D21}^{ij}\|w^e\| + L_{D22}^{ij}\|\varphi^e\| + L_{D23}^{ij}\|\psi^e\|\right)\right], \quad (30)
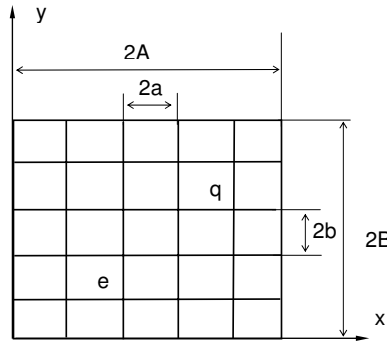\end{aligned}
$$

Figure 3. Boundary element mesh for a rectangular crack.

$$B_z^e = \sum_{i=1}^{4} \left[\left(-L_{B1}^i \bar{G}_{ii}^{(4)} + \sum_{j=1}^{4} L_{B2}^{ij} G_{ij}^{(4)} \right) \|u^e\| + \left(L_{B1}^i \bar{G}_{ii}^{(5)} + \sum_{j=1}^{4} L_{B2}^{ij} G_{ij}^{(5)} \right) \|v^e\| \right.$$
$$+ \bar{G}_{ii}^{(6)} \left(L_{B11}^i \|w^e\| + L_{B12}^i \|\varphi^e\| + L_{B13}^i \|\psi^e\| \right)$$
$$\left. + \sum_{j=1}^{4} G_{ij}^{(6)} \left(L_{B21}^{ij} \|w^e\| + L_{B22}^{ij} \|\varphi^e\| + L_{B23}^{ij} \|\psi^e\| \right) \right], \quad (31)$$

where the material related constants Ls and the functions Gs and $\bar{G}s$ with different superscripts and subscripts are given in Appendix B. These solutions are called extended Crouch fundamental solutions.

Equations (27)–(31) can be written in a compact form

$$\sigma_i^e = \sum_{j=1}^{5} F_{ij}^e \|u_j^e\|, \quad i, j = 1, 2, 3, 4, 5, \quad (32)$$

where $\sigma_1^e = \sigma_{xz}^e$, $\sigma_2^e = \sigma_{yz}^e$, $\sigma_3^e = \sigma_{zz}^e$, $\sigma_4^e = D_z^e$, $\sigma_5^e = B_z^e$, $\|u_1^e\| = \|u^e\|$, $\|u_2^e\| = \|v^e\|$, $\|u_3^e\| = \|w^e\|$, $\|u_4^e\| = \|\varphi^e\|$, $\|u_5^e\| = \|\psi^e\|$, and F_{ij}^e are called the influence functions of the rectangular element.

6. Extended displacement discontinuity method

If the domain of a crack is divided into N rectangular elements as shown in Figure 3 by using the extended Crouch fundamental solutions, the extended stress at the centroid of element q can be obtained by superposing the contribution of all the elements. Then, introducing the boundary conditions on the crack faces, one has

$$\sum_{e=1}^{N} \sum_{j=1}^{5} F_{ij}^e(x_q - x_e, y_q - y_e, z_q - z_e) \|u_i^e\| = \sigma_i^0(q), \quad q = 1, 2, 3, \ldots, N, \quad (33)$$

where σ_i^0 is related to the applied extended loading on the crack faces

$$
\begin{aligned}
p_x(x, y) &= -\sigma_1^0(x, y), \quad p_y(x, y) = -\sigma_2^0(x, y), \\
p_z(x, y) &= -\sigma_3^0(x, y), \quad \omega(x, y) = -\sigma_4^0(x, y), \\
\gamma(x, y) &= -\sigma_5^0(x, y).
\end{aligned}
\tag{34}
$$

Solving Equation (33), one obtains the extended displacement discontinuities on the crack faces. Furthermore, the extended stresses at any point in the crack plane can be calculated by

$$
\sigma_i(x, y, h) = \sum_{e=1}^{N} \sum_{j=1}^{5} F_{ij}^e(x - x_e, y - y_e, 0) \|u_j^e\|.
\tag{35}
$$

Finally, the extended stress intensity factors are calculated in [Zhao et al. 1997b; Zhao et al. 1998]:

$$
K_I^F = \lim_{\rho \to 0} \sqrt{2\pi\rho}\,\sigma_{zz}, \qquad K_I^D = \lim_{\rho \to 0} \sqrt{2\pi\rho}\,D_z, \quad K_I^B = \lim_{\rho \to 0} \sqrt{2\pi\rho}\,B_z,
\tag{36}
$$

where ρ is the distance from the crack tip.

7. Numerical examples and discussions

Consider a rectangular crack of sides $2A \times 2B$ at plane $z = h$ centered at point $(0, 0, h)$, with the sides parallel to the x- or y-axis. The magnetoelectroelastic medium is made of BaTiO$_3$ as the inclusion with CoFe$_2$O$_4$ as the matrix. The piezoelectric volume fraction of the inclusion is denoted by V_i. The material constants are given as follows [Huang et al. 1998]:

BaTiO$_3$:

$$
\begin{aligned}
c_{11} &= 166\,\text{GPa}, & c_{33} &= 162\,\text{GPa}, \\
c_{44} &= 43\,\text{GPa}, & c_{12} &= 77\,\text{GPa}, \\
c_{13} &= 78\,\text{GPa}, & e_{31} &= -4.4\,\text{C/m}^2, \\
e_{33} &= 18.6\,\text{C/m}^2, & e_{15} &= 11.6\,\text{C/m}^2, \\
\varepsilon_{11} &= 11.2 \times 10^{-9}\,\text{C}^2/(\text{Nm}^2), & \varepsilon_{33} &= 12.6 \times 10^{-9}\,\text{C}^2/(\text{Nm}^2), \\
\mu_{11} &= 5.0 \times 10^{-6}\,\text{Ns}^2/\text{C}^2, & \mu_{33} &= 10.0 \times 10^{-6}\,\text{Ns}^2/\text{C}^2.
\end{aligned}
\tag{37}
$$

CoFe$_2$O$_4$:

$$
\begin{aligned}
c_{11} &= 286\,\text{GPa}, & c_{33} &= 269.5\,\text{GPa}, \\
c_{44} &= 45.3\,\text{GPa}, & c_{12} &= 173.0\,\text{GPa}, \\
c_{13} &= 170.5\,\text{GPa}, & f_{31} &= 580.3\,\text{N/(Am)}, \\
f_{33} &= 699.7\,\text{N/(Am)}, & f_{15} &= 550.\,\text{N/(Am)}, \\
\varepsilon_{11} &= 0.08 \times 10^{-9}\,\text{C}^2/(\text{Nm}^2), & \varepsilon_{33} &= 0.093 \times 10^{-9}\,\text{C}^2/(\text{Nm}^2), \\
\mu_{11} &= 590 \times 10^{-6}\,\text{Ns}^2/\text{C}^2, & \mu_{33} &= 157 \times 10^{-6}\,\text{Ns}^2/\text{C}^2.
\end{aligned}
\tag{38}
$$

The following mixture rule is used to determine the composite material constants corresponding to the inclusion and matrix [Song and Sih 2003]

$$\Lambda^c = \Lambda^i V_i + \Lambda^m (1 - V_i), \tag{39}$$

where the superscripts "c", "i", and "m" represent the composite, inclusion, and matrix respectively. The two-phase transversely isotropic magnetoelectroelastic medium is obtained by assigning two different values of V_i in the upper and lower half-space, which are denoted by V_i^+ and V_i^-, respectively.

It should be pointed out that the value of μ_{11} used in [Huang et al. 1998] was negative. However, the negative value is questionable because it causes a negative internal energy and the Stroh formalism cannot be applied [Pan 2002]. The handbook, [Neelakanta 1995], indicates that the magnetic permeability of ferromagnetic materials, such as $CoFe_2O_4$, should be positive. Therefore, positive values were used in recent research [Sih et al. 2003]. Recently, this issue was discussed by [Chue and Liu 2005]. For these reasons, a positive value is also assigned to μ_{11} in the numerical calculations in the present paper.

Under the electrically and magnetically impermeable boundary condition, the uniformly distributed extended loadings on the crack faces are

$$p_x = 0, \qquad p_y = 0, \qquad p_z = 100\,\text{MPa}, \qquad \omega = 0.1\,\text{C/m}^2, \qquad \gamma = 10/\text{Am}. \tag{40}$$

The extended displacement discontinuity method is used to analyze the problem. The rectangular crack is divided into N rectangular elements of the same size. In order to decide the appropriate value of the element number N, we first consider a square crack far away from the interface, that is, the crack is in a homogeneous medium. The numerical calculations demonstrate that the maximum normalized intensity factors are the same and equal to 0.8072 when the element number $N = 81$. When $N = 225$ and $N = 625$, the values of maximum normalized intensity factors are 0.7928 and 0.7914, respectively. The normalized extended intensity factors F are given by

$$F_F = K_I^F / (\sqrt{\pi B}\sigma_z^0), \qquad F_D = K_I^D / (\sqrt{\pi B}D_z^0), \qquad F_B = K_I^F / (\sqrt{\pi B}B_z^0). \tag{41}$$

Though the convergence is not very fast, the difference of the maximum normalized intensity factors is less than 4% compared with that of purely elastic material in [Murkami 1992]. So the value $N = 225$ is used in the present paper for numerical analysis.

Figure 4 shows the normalized intensity factors along the crack front $\{0 < x < A, y = 0, z = h\}$ for different ratio of A/B. The larger the ratio of A/B is, the larger the normalized intensity factors are. The numerical results show that the extended intensity factors take the maximum value at the middle point $(A, 0, h)$. The most important finding is that the three normalized intensity factors become different due to the interface, which is unlike the case of a crack in a homogeneous medium [Zhao et al. 2006b].

Plotted in Figure 5 are the maximum normalized intensity factors versus $h/(2A)$ for different ratios of A/B. The three normalized intensity factors increase with the increase of A/B. When the ratio of $h/(2A)$ is larger than 1.0, the three maximum normalized extended stress intensity factors approach the same value for a given ratio of A/B. It shows the influence of the interface can be neglected and the crack can be considered in a homogeneous medium.

Figure 6 displays the normalized intensity factors versus x/A for different volume fractions V_i^- and $A/B = 1$. It can be seen that the stress and the magnetic induction intensity factors increase as x/A and
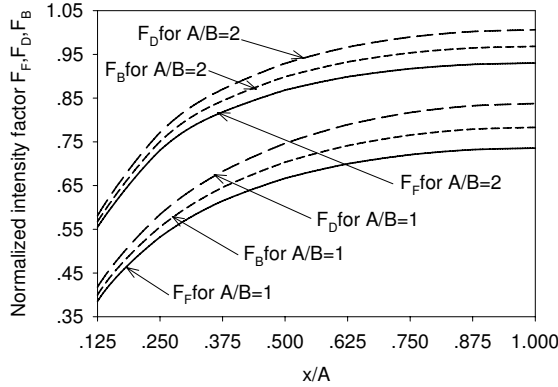
Figure 4. Normalized intensity factor F versus x/A with A/B for $V_i^+ = 0.5$, $V_i^- = 0.3$ and $h/(2A) = 0.2$.
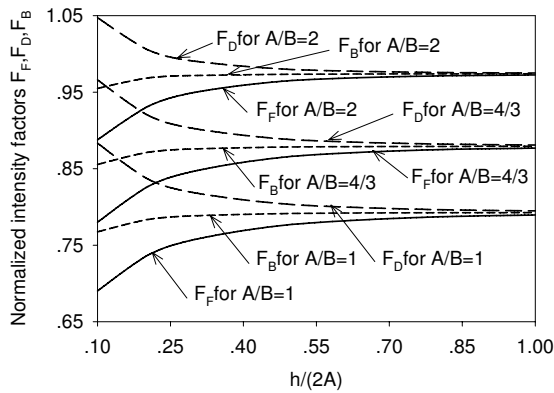
Figure 5. The maximum normalized intensity factor F versus $h/(2A)$ for $V_i^+ = 0.5$, $V_i^- = 0.3$ and different value of A/B.
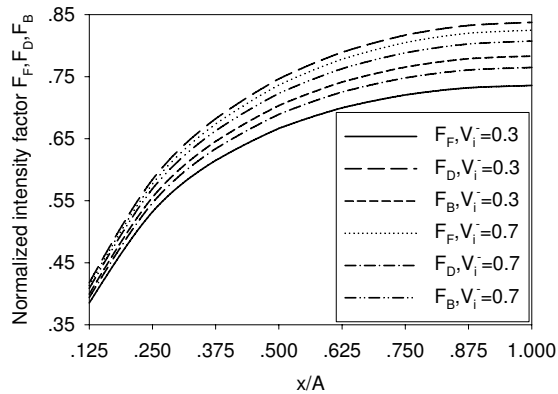
Figure 6. Normalized intensity factors F versus x/A with V_i^- for $V_i^+ = 0.5$, $h/(2A) = 0.2$ and $A/B = 1$.
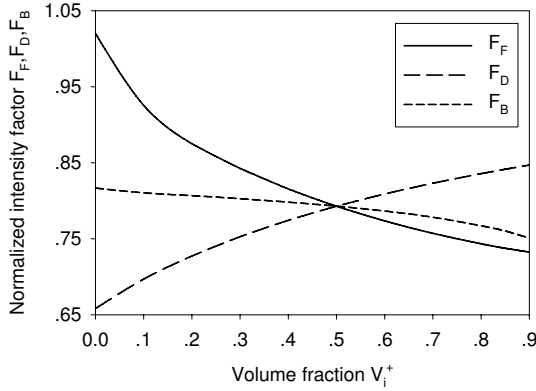
Figure 7. The maximum normalized intensity factors F versus V_i^+ for $h/(2A) = 0.2$, $V_i^- = 0.5$ and $A/B = 1$.

V_i^- increase, but the electric displacement intensity factors decrease as V_i^- increase. The normalized intensity factors take the maximum value at the middle point $(A, 0, h)$ independent of the volume fraction.

The maximum normalized intensity factors versus V_i^+ are depicted in Figure 7. It shows that the maximum stress and magnetic induction intensity factors decrease, while the maximum electric displacement intensity factors increase with the volume fraction V_i^+ increasing. The opposite trends are shown in Figure 8 for variation of V_i^-. It is interesting to note that the three maximum normalized intensity factors are the same when V_i^+ is equal to V_i^-, in which case the medium becomes homogeneous.

8. Concluding remarks

The displacement discontinuity method proposed by Crouch is extended to analyze cracks in three-dimensional two-phase transversely isotropic magnetoelectroelastic media. The numerical results of rectangular cracks show that the extended method is very efficient.
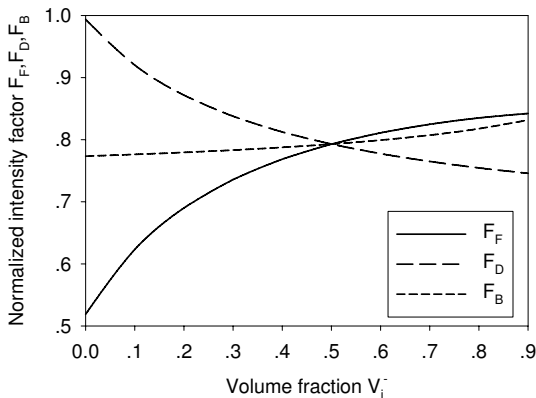

Figure 8. The maximum normalized intensity factors F versus V_i^- for $h/(2A) = 0.2$, $V_i^+ = 0.5$ and $A/B = 1$.

The three normalized intensity factors are equal for a crack in a homogeneous medium under the electrically and magnetically impermeable crack condition. For a crack in a two-phase medium, however, the three normalized intensity factors are unequal and greatly influenced by the size and the location of the crack and the material properties. This demonstrates that the crack behavior in an inhomogeneous magnetoelectroelastic material is very complicated under combined mechanical-electrical-magnetic loadings.

Although various models, such as the strip polarization saturation model, charge-free zone model, etc., were proposed [Zhang et al. 2002], a linear analysis is the first and most fundamental step toward understanding the fracture behaviors of piezoelectric materials, and the intensity factors are the fundamental parameters in these nonlinear models. Until now, the problem hasn't been solved completely. The fracture behavior of magnetoelectroelastic materials under combined mechanical-electrical-magnetic loading is more complicated than that of piezoelectric materials under combined mechanical-electrical loading. There is a long way yet to go to completely solve this problem.

Appendix A: Fundamental solutions

With regard to the problem of a point force, point charge, and point electric current applied at the point $(0, 0, h)$ in the interior of a two-phase transversely isotropic magnetoelectroelastic media with the interface being parallel to the plane of isotropy, a Cartesian coordinate system is chosen such that the xoy-plane lies in the interface.

The following material related constants will be used in the fundamental solutions:

$$
\begin{aligned}
\alpha_{im} &= k_{mi}s_i, \quad i = 1, 2, 3, 4, \quad m = 1, 2, 3, \\
\xi_i &= (c_{13}\alpha_{i1} + e_{31}\alpha_{i2} + f_{31}\alpha_{i3})s_i - c_{12}, \\
\omega_{51} &= c_{44}s_5, \\
\omega_{52} &= e_{15}s_5, \\
\omega_{53} &= f_{15}s_5, \\
\vartheta_{i1} &= (c_{33}\alpha_{i1} + e_{33}\alpha_{i2} + f_{33}\alpha_{i3})s_i - c_{13}, \\
\vartheta_{i2} &= (e_{33}\alpha_{i1} - \varepsilon_{33}\alpha_{i2} - g_{33}\alpha_{i3})s_i - e_{31}, \\
\vartheta_{i3} &= (f_{33}\alpha_{i1} - g_{33}\alpha_{i2} - \mu_{33}\alpha_{i3})s_i - f_{31}, \\
\omega_{i1} &= c_{44}(s_i + \alpha_{i1}) + e_{15}\alpha_{i2} + f_{15}\alpha_{i3}, \\
\omega_{i2} &= e_{15}(s_i + \alpha_{i1}) - \varepsilon_{11}\alpha_{i2} - g_{11}\alpha_{i3}, \\
\omega_{i3} &= f_{15}(s_i + \alpha_{i1}) - g_{11}\alpha_{i2} - \mu_{11}\alpha_{i3},
\end{aligned}
\tag{A.1}
$$

where s_i are the roots of the material characteristic equation and k_{mi} are the material related constants given in [Zhao et al. 2006b].

A.1. *Fundamental solutions corresponding to unit point force P_3 in the z-direction.* Using the derivation procedures of [Ding et al. 2005], the fundamental solutions are obtained.

When $z \geq 0$, we have

$$\tau_{xm} = P_3 x \sum_{i=1}^{4} \omega_{im} \left(\frac{A_i}{\bar{R}_{ii}^3} - \sum_{j=1}^{4} \frac{A_{ij}}{R_{ij}^3} \right), \qquad \tau_{ym} = P_3 y \sum_{i=1}^{4} \omega_{im} \left(\frac{A_i}{\bar{R}_{ii}^3} - \sum_{j=1}^{4} \frac{A_{ij}}{R_{ij}^3} \right),$$

$$\sigma_m = P_3 \sum_{i=1}^{4} \vartheta_{im} \left(\frac{A_i \bar{z}_{ii}}{\bar{R}_{ii}^3} - \sum_{j=1}^{4} \frac{A_{ij} z_{ij}}{R_{ij}^3} \right), \tag{A.2}$$

and when $z \leq 0$,

$$\tau'_{xm} = P_3 x \sum_{i=1}^{4} \sum_{j=1}^{4} \omega'_{im} \frac{A'_{ij}}{R_{ij}^{'3}}, \quad \tau'_{ym} = P_3 y \sum_{i=1}^{4} \sum_{j=1}^{4} \omega'_{im} \frac{A'_{ij}}{R_{ij}^{'3}}, \quad \sigma'_m = P_3 \sum_{i=1}^{4} \sum_{j=1}^{4} \vartheta'_{im} \frac{A'_{ij} z'_{ij}}{R_{ij}^{'3}}, \tag{A.3}$$

where variables with a prime refer to the half-space $z \leq 0$ and those without a prime correspond to the half-space $z \geq 0$. The related coefficients are determined by

$$\sum_{i=1}^{4} A_i = 0, \qquad\qquad 4\pi \sum_{i=1}^{4} \vartheta_{i1} A_i = -1,$$

$$4\pi \sum_{i=1}^{4} \vartheta_{i2} A_i = 0, \qquad\qquad 4\pi \sum_{i=1}^{4} \vartheta_{i3} A_i = 0,$$

$$A_i + \sum_{j=1}^{4} A_{ji} = \sum_{j=1}^{4} A'_{ji}, \qquad A_i \alpha_{im} - \sum_{j=1}^{4} A_{ji} \alpha_{jm} = \sum_{j=1}^{4} A'_{ji} \alpha'_{jm}, \tag{A.4}$$

$$A_i \vartheta_{im} + \sum_{j=1}^{4} A_{ji} \vartheta_{jm} = \sum_{j=1}^{4} A'_{ji} \vartheta'_{jm}, \qquad A_i \omega_{i1} - \sum_{j=1}^{4} A_{ji} \omega_{j1} = \sum_{j=1}^{4} A'_{ji} \omega'_{j1}.$$

Solutions corresponding to the unit point charge P_4 and point current P_5 are in the same form as Equations (A.2)–(A.4), but P_3 and A_i should be replaced respectively by P_4 and B_i and P_5 and C_i. The coefficients B_i and C_i are determined by

$$\sum_{i=1}^{4} B_i = 0, \qquad\qquad 4\pi \sum_{i=1}^{4} \vartheta_{i1} B_i = 0,$$

$$4\pi \sum_{i=1}^{4} \vartheta_{i2} B_i = 1, \qquad\qquad 4\pi \sum_{i=1}^{4} \vartheta_{i3} B_i = 0,$$

$$B_i + \sum_{j=1}^{4} B_{ji} = \sum_{j=1}^{4} B'_{ji}, \qquad B_i \alpha_{im} - \sum_{j=1}^{4} B_{ji} \alpha_{jm} = \sum_{j=1}^{4} B'_{ji} \alpha'_{jm}, \tag{A.5}$$

$$B_i \vartheta_{im} + \sum_{j=1}^{4} B_{ji} \vartheta_{jm} = \sum_{j=1}^{4} B'_{ji} \vartheta'_{jm}, \qquad B_i \omega_{i1} - \sum_{j=1}^{4} B_{ji} \omega_{j1} = \sum_{j=1}^{4} B'_{ji} \omega'_{j1},$$

$$\sum_{i=1}^{4} C_i = 0, \qquad\qquad 4\pi \sum_{i=1}^{4} \vartheta_{i1} C_i = 0,$$

$$4\pi \sum_{i=1}^{4} \vartheta_{i2} C_i = 0, \qquad\qquad 4\pi \sum_{i=1}^{4} \vartheta_{i3} C_i = 1, \tag{A.6}$$

$$C_i + \sum_{j=1}^{4} C_{ji} = \sum_{j=1}^{4} C'_{ji}, \qquad\qquad C_i \alpha_{im} - \sum_{j=1}^{4} C_{ji} \alpha_{jm} = \sum_{j=1}^{4} C'_{ji} \alpha'_{jm},$$

$$C_i \vartheta_{im} + \sum_{j=1}^{4} C_{ji} \vartheta_{jm} = \sum_{j=1}^{4} C'_{ji} \vartheta'_{jm}, \qquad\qquad C_i \omega_{i1} - \sum_{j=1}^{4} C_{ji} \omega_{j1} = \sum_{j=1}^{4} C'_{ji} \omega'_{j1}.$$

A.2. *Fundamental solutions corresponding to unit point force P_1 in the x-direction.* When $z \geq 0$, the fundamental solutions are given by

$$\tau_{xm} = -P_1 \omega_{5m} \left[D_5 \left(\frac{1}{\bar{R}_{55}(\bar{R}_{55} - \bar{z}_{55})} - \frac{y^2}{\bar{R}_{55}^3(\bar{R}_{55} - \bar{z}_{55})} - \frac{y^2}{\bar{R}_{55}^2(\bar{R}_{55} - \bar{z}_{55})^2} \right) \right.$$

$$\left. - D_{55} \left(\frac{1}{R_{55}(R_{55} + z_{55})} - \frac{y^2}{R_{55}^3(R_{55} + z_{55})} - \frac{y^2}{R_{55}^2(R_{55} + z_{55})^2} \right) \right]$$

$$+ P_1 \sum_{i=1}^{4} \omega_{im} \left[D_i \left(\frac{1}{\bar{R}_{ii}(\bar{R}_{ii} - \bar{z}_{ii})} - \frac{x^2}{\bar{R}_{ii}^3(\bar{R}_{ii} - \bar{z}_{ii})} - \frac{x^2}{\bar{R}_{ii}^2(\bar{R}_{ii} - \bar{z}_{ii})^2} \right) \right.$$

$$\left. - \sum_{j=1}^{4} D_{ij} \left(\frac{1}{R_{ij}(R_{ij} + z_{ij})} - \frac{x^2}{R_{ij}^3(R_{ij} + z_{ij})} - \frac{x^2}{R_{ij}^2(R_{ij} + z_{ij})^2} \right) \right],$$

$$\tau_{ym} = -\omega_{5m} P_1 xy \left[D_5 \left(\frac{1}{\bar{R}_{55}^3(\bar{R}_{55} - \bar{z}_{55})} + \frac{1}{\bar{R}_{55}^2(\bar{R}_{55} - \bar{z}_{55})^2} \right) \right.$$

$$\left. - \sum_{j=1}^{4} D_{55} \left(\frac{1}{R_{55}^3(R_{55} + z_{55})} + \frac{1}{R_{55}^2(R_{55} + z_{55})^2} \right) \right]$$

$$- P_1 xy \sum_{i=1}^{4} \omega_{im} \left[D_i \left(\frac{1}{\bar{R}_{ii}^3(\bar{R}_{ii} - \bar{z}_{ii})} + \frac{1}{\bar{R}_{ii}^2(\bar{R}_{ii} - \bar{z}_{ii})^2} \right) \right.$$

$$\left. - \sum_{j=1}^{4} D_{ij} \left(\frac{1}{R_{ij}^3(R_{ij} + z_{ij})} + + \frac{1}{R_{ij}^2(R_{ij} + z_{ij})^2} \right) \right],$$

$$\sigma_m = P_1 x \sum_{i=1}^{4} \vartheta_{im} \left[\frac{D_i}{\bar{R}_{ii}^3} + \sum_{i=1}^{4} \frac{D_{ij}}{R_{ij}^3} \right],$$

and when $z \leq 0$

$$\tau'_{xm} = -P_1 \omega'_{5m} D'_{55} \left[\frac{1}{R'_{55}(R'_{55} - z'_{55})} - \frac{y^2}{R'^3_{55}(R'_{55} - z'_{55})} - \frac{y^2}{R'^2_{55}(R'_{55} - z'_{55})^2} \right]$$

$$+ P_1 \sum_{i=1}^{4} \sum_{j=1}^{4} D'_{ij} \omega'_{im} \left[\frac{1}{R'_{ij}(R'_{ij} - z'_{ij})} - \frac{x^2}{R'^3_{ij}(R'_{ij} - z'_{ij})} - \frac{x^2}{R'^2_{ij}(R'_{ij} - z'_{ij})^2} \right],$$

$$\tau'_{ym} = -P_1 \omega'_{5m} D'_{55} xy \left[\frac{1}{R'^3_{55}(R'_{55} - z'_{55})} + \frac{1}{R'^2_{55}(R'_{55} - z'_{55})^2} \right]$$

$$- P_1 \sum_{i=1}^{4} \sum_{j=1}^{4} D'_{ij} \omega'_{im} xy \left[\frac{1}{R'^3_{ij}(R'_{ij} - z'_{ij})} + \frac{1}{R'^2_{ij}(R'_{ij} - z'_{ij})^2} \right],$$

$$\sigma'_m = P_1 x \sum_{i=1}^{4} \sum_{j=1}^{4} \vartheta'_{im} \frac{D'_{ij}}{R'^3_{ij}},$$

where the coefficients D_i, D_{ij}, D'_{ij} are given by

$$\sum_{i=1}^{4} \alpha_{im} D_i = 0, \qquad s_5 D_5 + \sum_{i=1}^{4} s_i D_i = 0,$$

$$2\pi c_{44} s_5 D_5 - 2\pi \sum_{i=1}^{4} \omega_{i1} D_i = -1, \qquad D_5 + D_{55} = D'_{55},$$

$$\alpha_{im} D_i - \sum_{j=1}^{4} \alpha_{jm} D_{ji} = \sum_{j=1}^{4} \alpha'_{jm} D'_{ji}, \qquad D_i + \sum_{j=1}^{4} D_{ji} = \sum_{j=1}^{4} D'_{ji},$$

$$\omega_{51}(D_{55} - D_5) = -\omega'_{51} D'_{55}, \qquad \omega_{i1} D_i - \sum_{j=1}^{4} \omega_{j1} D_{ji} = \sum_{j=1}^{4} \omega'_{j1} D'_{ji},$$

$$\vartheta_{im} D_i + \sum_{j=1}^{4} \vartheta_{jm} D_{ji} = \sum_{j=1}^{4} \vartheta'_{jm} D'_{jm}.$$

By simple coordinate transformation, solutions to the problem of unit point force P_2 in the y-direction can be easily obtained from the above solutions.

Appendix B: The constants Ls and the functions Gs and $\bar{G}s$

The coefficients in Equations (27)–(31) are given by

$$Q_i^1 = D_i s_i c_{44} + c_{44} A_i - e_{15} B_i - f_{15} C_i, \qquad Q_i^2 = c_{13} D_i - s_i(c_{33} A_i - e_{33} B_i - f_{33} C_i), \qquad \text{(B.1)}$$

$$Q_i^3 = e_{31} D_i - s_i(e_{33} A_i + \varepsilon_{33} B_i + g_{33} C_i), \qquad Q_i^4 = f_{31} D_i - s_i(f_{33} A_i + g_{33} B_i + \mu_{33} C_i),$$

$$L_{X1} = c_{44}\omega_{51}s_5 D_5, \qquad\qquad L_{X2} = c_{44}\omega_{51}s_5 D_{55},$$

$$L_{11}^i = \omega_{i1} Q_i^1, \qquad\qquad L_{21k}^i = \vartheta_{ik} Q_i^1,$$

$$L_{Z1}^i = \omega_{i1} Q_i^2, \qquad\qquad L_{Z1k}^i = \vartheta_{ik} Q_i^2, \tag{B.2}$$

$$L_{D1}^i = \omega_{i1} Q_i^3, \qquad\qquad L_{D1k}^i = \vartheta_{ik} Q_i^3,$$

$$L_{B1}^i = \omega_{i1} Q_i^4, \qquad\qquad L_{B1k}^i = \vartheta_{ik} Q_i^4, \quad k = 1, 2, 3.$$

The coefficients

$$L_{12}^{ij}, L_{22k}^{ij}, L_{Z2}^{ij}, L_{Z2k}^{ij}, L_{D2}^{ij}, L_{D2k}^{ij}, L_{B2}^{ij}, \text{ and } L_{B2k}^{ij}$$

can be obtained correspondingly by taking

$$s_j, A_{ij}, B_{ij}, C_{ij}, \text{ and } D_{ij}$$

instead of s_i, A_i, B_i, C_i, and D_i in the above equations, respectively.

And the functions $\bar{G}$s with different superscripts and subscripts are given by

$$\bar{G}_{ii}^{(1)} = \frac{b-y}{(b-y)^2+\bar{z}_{ii}^2}\left(\frac{a-x}{\sqrt{(a-x)^2+(b-y)^2+\bar{z}_{ii}^2}} + \frac{a+x}{\sqrt{(x+a)^2+(b-y)^2+\bar{z}_{ii}^2}}\right)$$
$$+ \frac{b+y}{(b+y)^2+\bar{z}_{ii}^2}\left(\frac{a-x}{\sqrt{(a-x)^2+(b+y)^2+\bar{z}_{ii}^2}} + \frac{a+x}{\sqrt{(x+a)^2+(b+y)^2+\bar{z}_{ii}^2}}\right),$$

$$\bar{G}_{ii}^{(3)} = \frac{1}{\sqrt{(a-x)^2+(b-y)^2+\bar{z}_{ii}^2}} - \frac{1}{\sqrt{(a+x)^2+(b-y)^2+\bar{z}_{ii}^2}}$$
$$- \frac{1}{\sqrt{(a-x)^2+(b+y)^2+\bar{z}_{ii}^2}} + \frac{1}{\sqrt{(a+x)^2+(b+y)^2+\bar{z}_{ii}^2}},$$

$$\bar{G}_{ii}^{(4)} = \frac{1}{(a-x)^2+\bar{z}_{ii}^2}\left(\frac{b-y}{\sqrt{(a-x)^2+(b-y)^2+\bar{z}_{ii}^2}} + \frac{b+y}{\sqrt{(a-x)^2+(b+y)^2+\bar{z}_{ii}^2}}\right)$$
$$- \frac{1}{(a+x)^2+\bar{z}_{ii}^2}\left(\frac{b-y}{\sqrt{(a+x)^2+(b-y)^2+\bar{z}_{ii}^2}} + \frac{b+y}{\sqrt{(a+x)^2+(b+y)^2+\bar{z}_{ii}^2}}\right),$$

$$\bar{G}_{ii}^{(6)} = \frac{(y-b)(a-x)}{\sqrt{(a-x)^2+(b-y)^2+\bar{z}_{ii}^2}}\left(\frac{1}{(b-y)^2+\bar{z}_{ii}^2} + \frac{1}{(a-x)^2+\bar{z}_{ii}^2}\right)$$
$$+ \frac{(y-b)(a+x)}{\sqrt{(a+x)^2+(b-y)^2+\bar{z}_{ii}^2}}\left(\frac{1}{(b-y)^2+\bar{z}_{ii}^2} + \frac{1}{(a+x)^2+\bar{z}_{ii}^2}\right)$$

$$-\frac{(y+b)(a-x)}{\sqrt{(a-x)^2+(b+y)^2+\bar{z}_{ii}^2}}\left(\frac{1}{(b+y)^2+\bar{z}_{ii}^2}+\frac{1}{(a-x)^2+\bar{z}_{ii}^2}\right)$$

$$-\frac{(y+b)(a+x)}{\sqrt{(a+x)^2+(b+y)^2+\bar{z}_{ii}^2}}\left(\frac{1}{(b+y)^2+\bar{z}_{ii}^2}+\frac{1}{(a+x)^2+\bar{z}_{ii}^2}\right).$$

The functions $\bar{G}_{ii}^{(2)}$ and $\bar{G}_{ii}^{(5)}$ can be obtained respectively from $\bar{G}_{ii}^{(1)}$ and $\bar{G}_{ii}^{(4)}$ by taking a, b, x, and y instead of b, a, y, and x, respectively. The functions Gs can be obtained by taking z_{ij} instead of $\bar{z}_{ii}$ in $\bar{G}s$.

References

[Chue and Liu 2005] C. H. Chue and T. J. C. Liu, "Magneto-electro-elastic antiplane analysis of a bimaterial BaTiO3-CoFe2O4 composite wedge with an interface crack", *Theor. Appl. Fract. Mec.* **44**:3 (2005), 275–296.

[Chung and Ting 1995] M. Y. Chung and T. C. T. Ting, "The Green function for a piezoelectric piezomagnetic anisotropic elastic medium with an elliptic hole or rigid inclusion", *Phil. Mag.* **72** (1995), 405–410.

[Crouch 1976] S. L. Crouch, "Solution of plane elasticity problems by the displacement discontinuity method", *Int. J. Numer. Meth. Eng.* **10**:2 (1976), 301–343.

[Ding et al. 2005] H. Ding, A. Jiang, P. Hou, and W. Chen, "Green's functions for two-phase transversely isotropic magneto-electro-elastic media", *Eng. Anal. Bound. Elem.* **29**:6 (2005), 551–561.

[Gao and Noda 2004] C.-F. Gao and N. Noda, "Thermal-induced interfacial cracking of magnetoelectroelastic materials", *Int. J. Eng. Sci.* **42**:13-14 (2004), 1347–1360.

[Hou et al. 2005] P.-F. Hou, H.-J. Ding, and J.-Y. Chen, "Green's functions for transversely isotropic magnetoelectroelastic media", *Int. J. Eng. Sci.* **43**:10 (2005), 826–858.

[Huang and Kuo 1997] J. H. Huang and W.-S. Kuo, "The analysis of piezoelectric/piezomagnetic composite materials containing an ellipsoidal inclusion", *J. Appl. Phys.* **81**:3 (1997), 1378–1386.

[Huang et al. 1998] J. H. Huang, Y.-H. Chiu, and H.-K. Liu, "Magneto-electro-elastic eshelby tensors for a piezoelectric-piezomagnetic composite reinforced by ellipsoidal inclusions", *J. Appl. Phys.* **83**:10 (1998), 5364–5370.

[Jiang and Pan 2004] X. Jiang and E. Pan, "Exact solution for 2D polygonal inclusion problem in anisotropic magnetoelectroelastic full-, half-, and bimaterial-planes", *Int. J. Solids Struct.* **41**:16-17 (2004), 4361–4382.

[Liu and Liu 2001] J. Liu and Y. Liu, X.and Zhao, "Green's functions for anisotropic magnetoelectroelastic solids with an elliptical cavity or a crack", *Int. J. Eng. Sci.* **39**:12 (2001), 1405–1418.

[Murkami 1992] Y. Murkami, *Stress intensity factors handbook*, vol. 3, Pergamon, Oxford, 1992. v.3 published with the aid of The Society os Materials Science, Japan.

[Neelakanta 1995] P. S. Neelakanta, *Handbook of electromagnetic materials: monolithic and composite versions and their applications*, CRC Press, Boca Raton, FL, 1995.

[Pan 1991] E. Pan, "Dislocation in an infinite poroelastic medium", *Acta Mech.* **87**:1-2 (1991), 105–115.

[Pan 2002] E. Pan, "Three-dimensional Green's functions in anisotropic magneto-electro-elastic bimaterials", *Z. Angew. Math. Phys.* **53**:5 (2002), 815–838.

[Pan and Amadei 1996] E. Pan and B. Amadei, "Fracture mechanics analysis of cracked 2-D anisotropic media witha new formulation of the boundary element method", *Int. J. Fracture* **77**:2 (1996), 161–174.

[Qin 2004] Q. H. Qin, "Green's functions of magnetoelectroelastic solids with a half-plane boundary or bimaterial interface", *Phil. Mag.* **84**:12 (2004), 771–779.

[Sih et al. 2003] G. C. Sih, R. Jones, and Z. F. Song, "Piezomagnetic and piezoelectric poling effects on mode I and II crack initiation behavior of magnetoelectroelastic materials", *Theor. Appl. Fract. Mec.* **40**:2 (2003), 161–186.

[Song and Sih 2003] Z. F. Song and G. C. Sih, "Crack initiation behavior in magnetoelectroelastic composite under in-plane deformation", *Theor. Appl. Fract. Mec.* **39**:3 (2003), 189–207.

[Tian and Rajapakse 2005] W. Y. Tian and R. K. N. D. Rajapakse, "Fracture analysis of magnetoelectroelastic solids by using path independent integrals", *Int. J. Fracture* **131**:4 (2005), 311–335.

[Wang and Mai 2003] B. L. Wang and Y.-W. Mai, "Crack tip field in piezoelectric/piezomagnetic media", *Eur. J. Mech. A Solids* **22**:4 (2003), 591–602.

[Wang and Shen 2002] X. Wang and Y.-P. Shen, "The general solution of three-dimensional problems in magnetoelectroelastic media", *Int. J. Eng. Sci.* **40**:10 (2002), 1069–1080.

[Wang and Shen 2003] X. Wang and Y.-P. Shen, "Inclusions of arbitrary shape in magnetoelectroelastic composite materials", *Int. J. Eng. Sci.* **41**:1 (2003), 85–102.

[Wen 1996] P. H. Wen, *Dynamic fracture mechanics: displacement discontinuity method*, vol. 29, Topic in Engineering, Computational Mechanics Publications, Boston, 1996.

[Zhang et al. 2002] T. Y. Zhang, M. H. Zhao, and P. Tong, "Fracture of piezoelectric ceramics", *Adv. Appl. Mech.* **38** (2002), 147–289.

[Zhao et al. 1997a] M. H. Zhao, Y. P. Shen, Y. J. Liu, and G. N. Liu, "Isolated crack in three-dimensional piezoelectric solid, I: solution by Hankel transform", *Theor. Appl. Fract. Mec.* **26**:2 (1997), 129–139.

[Zhao et al. 1997b] M. H. Zhao, Y. P. Shen, Y. J. Liu, and G. N. Liu, "Isolated crack in three-dimensional piezoelectric solid, II: stress intensity factors for circular crack", *Theor. Appl. Fract. Mec.* **26**:2 (1997), 141–149.

[Zhao et al. 1998] M. H. Zhao, Y. P. Shen, Y. J. Liu, and G. N. Liu, "The method of analysis of cracks in three-dimensional transversely isotropic media: boundary integral equation approach", *Eng. Anal. Bound. Elem.* **21**:2 (1998), 169–178.

[Zhao et al. 2004] M.-H. Zhao, P.-Z. Fang, and Y.-P. Shen, "Boundary integral-differential equations and boundary element method for interfacial cracks in three-dimensional piezoelectric media", *Eng. Anal. Bound. Elem.* **28**:7 (2004), 753–762.

[Zhao et al. 2006a] M. H. Zhao, H. Wang, F. Yang, and T. Liu, "A magnetoelectroelastic medium with an elliptical cavity under combined mechanical-electric-magnetic loading", *Theor. Appl. Fract. Mec.* **45**:3 (2006), 227–237.

[Zhao et al. 2006b] M. H. Zhao, F. Yang, and T. Liu, "Analysis of a penny-shaped crack in a magneto-electro-elastic medium", *Phil. Mag.* **86**:28 (2006), 4397–4416.

[Zhou et al. 2004] Z.-G. Zhou, B. Wang, and Y.-G. Sun, "Two collinear interface cracks in magneto-electro-elastic composites", *Int. J. Eng. Sci.* **42**:11-12 (2004), 1155–1167.

MINGHAO ZHAO: memhzhao@zzu.edu.cn
Department of Engineering Mechanics, Zhengzhou University, No. 100 Science Road, Zhengzhou, Henan Province 450001, China

NA LI: zhuofan8227@163.com
Department of Engineering Mechanics, Zhengzhou University, No. 100 Science Road, Zhengzhou, Henan Province 450001, China

CUIYING FAN: fcymaster@126.com
Department of Engineering Mechanics, Zhengzhou University, No. 100 Science Road, Zhengzhou, Henan Province 450001, China

TONG LIU: Liutung@zzu.edu.cn
Department of Engineering Mechanics, Zhengzhou University, No. 100 Science Road, Zhengzhou, Henan Province 450001, China